Microscopic origin of magnetic linear dichroism in the antiferromagnetic insulator MnF_2

Takuya Higuchi[1] and Makoto Kuwata-Gonokami[1,2]
[1]*Department of Physics, The University of Tokyo, 7-3-1 Hongo, Bunkyo-ku, Tokyo 113-0033, Japan*
[2]*Photon Science Center, The University of Tokyo, 7-3-1 Hongo, Bunkyo-ku, Tokyo 113-0086, Japan*
(Received 12 April 2013; published 10 June 2013)

Magnetically ordered crystals often show unique magneto-optical phenomena that are not found without magnetic order. For example, MnF_2, a two-sublattice antiferromagnet with different sublattice symmetries shows magnetic linear dichroism (MLD), which is odd with respect to the external magnetic field in the Faraday geometry. In particular, the magnon sideband of an exciton with a particular orbital function exhibits MLD, and the commonly found magnetic circular dichroism (MCD) is almost absent. In this study, we clarify the microscopic origin of this characteristic feature. We found that the symmetry of the exciton orbital determines the polarization eigenstate of the light to create the exciton magnon pair. These eigenstates can even be two cross-linear polarizations, depending in which sublattice the exciton is created. In this case, only MLD is allowed and MCD is forbidden.

DOI: 10.1103/PhysRevB.87.224405 PACS number(s): 76.50.+g, 87.64.ku, 71.35.Ji, 71.35.Gg

I. INTRODUCTION

Magneto-optical effects are widely used to probe the magnetic properties of various materials.[1,2] For example, when an external magnetic field **H** is applied to a medium, a difference in absorption coefficients for left and right circularly polarized light can be induced.[2] This is magnetic circular dichroism (MCD), and it is odd with respect to the field **H**. This is the direct consequence of Onsager's reciprocity relation for optical susceptibility, $\chi_{ij} = \theta\chi_{ji}$, where θ is the time-reversal operation.[3] When χ is written as a function of **H**, it should satisfy the relation $\chi_{ij}(\mathbf{H}) = \chi_{ji}(-\mathbf{H})$ because the magnetic field changes its sign under time reversal. Hence, the terms odd with respect to the magnetic field are antisymmetric under the interchange of the subscripts, which results in the MCD.

Magnetically ordered crystals sometimes show unique magneto-optical phenomena because the optical susceptibility can also be a function of magnetic order parameters. This happens when the time-reversal symmetry is broken macroscopically, i.e., even with any spatial translation. In terms of group theory, the magnetic point group of the crystal does not include θ alone as a symmetric operation.[4] In this case, the susceptibility tensor may have components that are odd with respect to the magnetic order parameter.[5] For example, consider a two-sublattice antiferromagnet with different site symmetries between the sublattices. The antiferromagnetic order parameter **L** is defined as the difference between the sublattice magnetizations. The Onsager's reciprocity relation gives $\chi_{ij}(\mathbf{H},\mathbf{L}) = \chi_{ji}(-\mathbf{H}, -\mathbf{L})$ because both **H** and **L** change their signs under time reversal. Therefore, the terms odd with respect to both **H** and **L** are symmetric under the interchange of subscripts. This results in magnetic linear dichroism (MLD),[5] the different absorption for the cross-linearly polarized waves propagating in the direction of the external magnetic field.

MnF_2, an antiferromagnetic insulator, is an example of a material that exhibits the MLD.[6] MnF_2 crystalizes in a rutile-like structure,[7] and the spins of the Mn^{2+} ions of the two sublattices align antiferromagnetically along its [001] axis (Fig. 1) below its Néel temperature of 67.7 K.[8] One can observe from Fig. 1 that the symmetries of the corner and the body-centered sites (Wyckoff positions of the space group $P4_2/mnm$) are different. Therefore, time-reversal symmetry is broken with any spatial translation. Indeed, the magnetic point group of MnF_2 in the antiferromagnetic phase is $4'/mmm'$, which does not include θ alone. This magnetic point group allows both the MLD and MCD, as was confirmed by Kharchenko *et al.*[6] They observed both the MLD and MCD at the following absorption resonances: (1) *A* line: ${}^6A_{1g} \rightarrow {}^4T_{1g}$; (2) *C* line: ${}^6A_{1g} \rightarrow ({}^4A_{1g}, {}^4E_g)$; and (3) *D* line: ${}^6A_{1g} \rightarrow {}^4T_{2g}$. They found that the MLD and MCD had similar shapes for the cases of the *A* and *D* lines. On the other hand, the MLD and MCD had very different shapes for the *C* line. Namely, the MCD around the magnon-sideband absorption is much weaker than MLD.

Note that the MCD was also observed by previous studies, and the difference between the MCD of the *A* line and *C* line was found. Scarpace *et al.* observed the MCD of the *A* line,[9] where the main features of the MCD spectra were well understood to be a result of Zeeman splitting of the magnon sidebands. On the other hand, Schwartz *et al.* observed the MCD of the *C* line,[10] where the MCD of magnetic-dipole resonance was observed, and the MCD of the magnon sideband was much smaller.

The origin of the dichroism spectra, in particular the characteristic behavior of those of the *C* line, remains an open question. This is partly because their microscopic origin has only been examined phenomenologically on the basis of the macroscopic symmetry arguments and because the systematic studies of their magnetic field dependence were not performed in the earlier studies. Although the MLD and MCD were clearly odd functions of the applied magnetic field, more systematic experiments were required to determine their origin.

To solve these problems, we performed systematic experimental and theoretical studies of dichroism in MnF_2 with an external magnetic field acting along its optical axis. We measured the magnetic field dependence of both the MLD and MCD of the *C* line precisely in order to determine their origin. Because various absorption lines (exciton lines and their magnon sidebands) overlap in this region, their behaviors under a varying magnetic field strength provide key information to help in separating their contributions to the MLD and MCD spectra. We then clarified why some magnon sidebands of the excitons in MnF_2 show MLD rather than MCD on the basis of a microscopic theory. In particular,

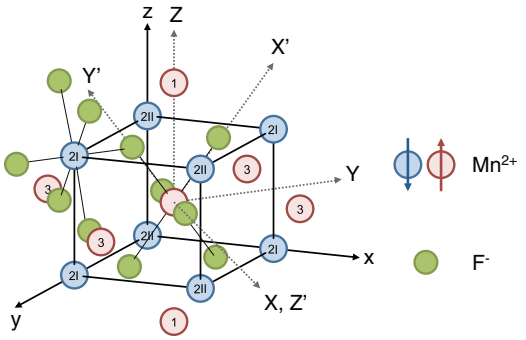

FIG. 1. (Color online) Crystal structure and spin alignment of MnF_2. Labels 1, 2, and 3 on Mn^{2+} indicate the first, second, and third neighbors of the centered ion, respectively. Labels 2I and 2II distinguish the two types of second neighbors. The Mn^{2+} ions are located at the center of an octahedra of F^- anions. Its site symmetry is almost O_h, and the slight distortion reduces it to D_{2h}. Three types of coordinates are described: (x,y,z) is the crystal coordinate, (X,Y,Z) is the site coordinate considering the site symmetry to be D_{2h} or the double group of C_{2h}, and (X',Y',Z') is used when it is taken as O_h.

we show that the polarization eigenstates needed to create an exciton magnon pair in MnF_2 can be two orthogonal linear polarizations under the external field, rather than two countercircular polarizations. These results allow us to explain the line shape of the MLD resonance, whose origins have not been well assigned in previous studies.[6]

II. EXPERIMENTAL OBSERVATIONS OF THE MLD AND MCD

Systematic measurements of the MLD and MCD spectra of the C line as functions of the external magnetic field were very helpful for investigating their origin. The amount of linear (circular) dichroism in the system was obtained by taking the difference between absorption coefficients for the X and Y (left- and right-circularly) polarized light, which were calculated from the transmission spectra. A light-emitting diode (LED) with a central wavelength of 398 nm and a bandwidth of 8 nm was employed as a light source. A single crystal of MnF_2 having a (001) face and a thickness of 1 mm was placed in the cryostat (MicrostatMO; Oxford instruments) and cooled to 10 K. The light transmitted through the specimen was then introduced into a monochromator (SpectraPro-300i; Acton Research), and the spectrum of the transmitted light was recorded by a charge-coupled device (CCD) based optical multichannel analyzer (LN/CCD-1100PG/UV; Princeton Instruments).

Figure 2(a) shows the measured absorption spectrum. In the near ultraviolet and visible regions, the optical response

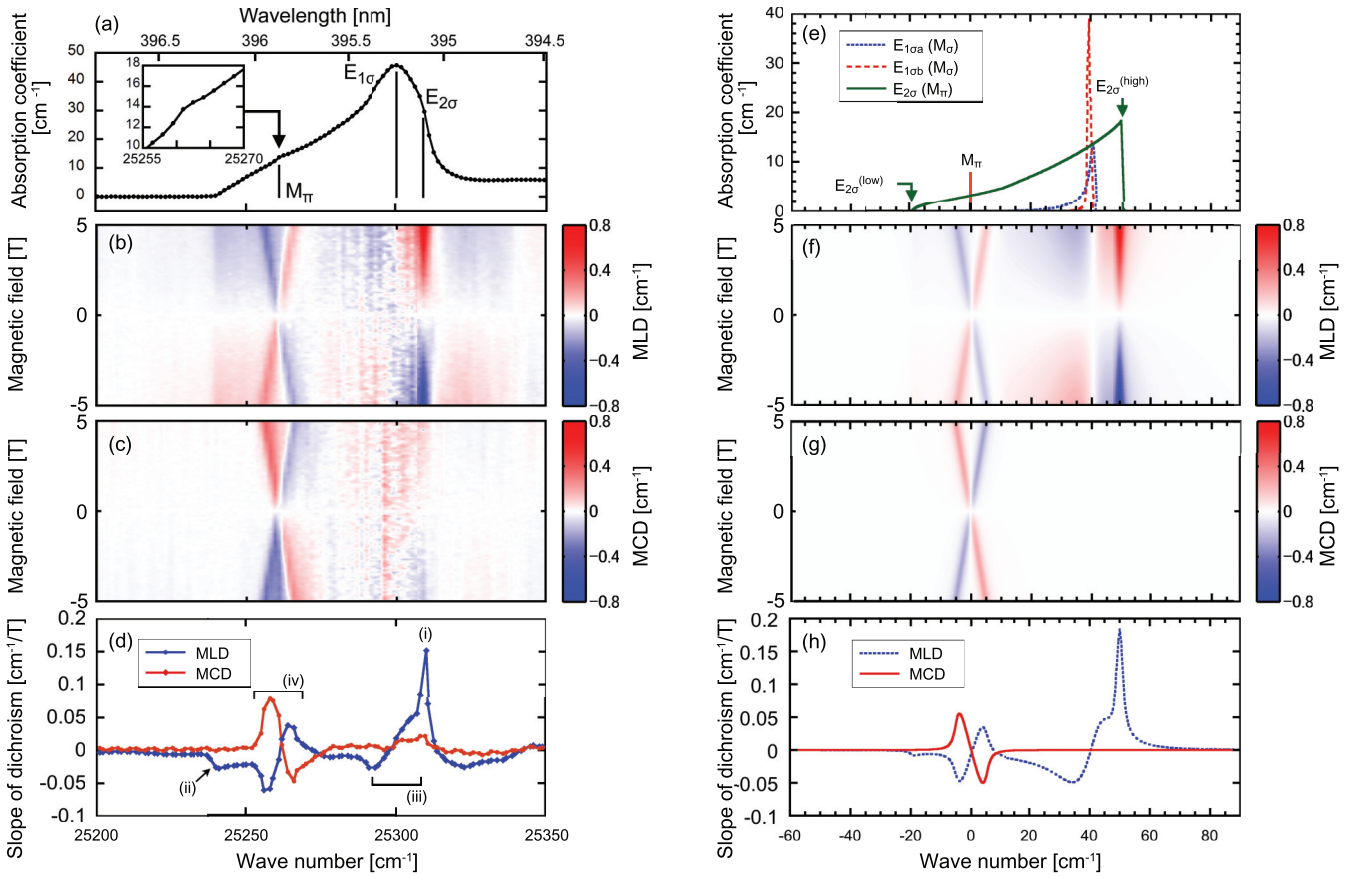

FIG. 2. (Color online) (a) Experimentally obtained absorption spectra. (b) The MLD and (c) the MCD as functions of the applied magnetic field, and (d) their slopes over the external field. Calculated spectra of (e) the absorption, (f) the MLD, (g) the MCD, and (h) their slopes over the field strength. For the calculation of the dichroism, phenomenological broadening was introduced to the absorption lines in the forms of Lorentzian functions: $[1+(\nu/\nu_0)^2]^{-1}$, and $\nu_0 = 14$, 2, and 3 cm^{-1} for $E_{1\sigma}$ [both (a) and (b)], $E_{2\sigma}$, and M_π, respectively.

of MnF_2 is dominated by intra-atomic excitations of manganese ions.[11,12] Because the Mn^{2+} ion takes a high-spin d^5 configuration as its ground state, the intra-atomic electronic excitation to a higher-energy d state (Frenkel exciton) has even parity and requires a spin flip. Therefore, the creation of an exciton via a process in which an electric dipole is allowed is doubly forbidden both in parity and spin. On the other hand, weak magnetic dipole transitions are allowed because they are mediated by the spin-orbit coupling.[13,14] In contrast, the collective excitation of an exciton and a magnon in different sublattices results in stronger electric dipole active transitions.[14–16] This pair creation forms a magnon sideband of an exciton, which dominates the optical-absorption spectra. A weak magnetic dipole transition line (M_π) at 25 262 cm^{-1} corresponds to the creation of an exciton, and its magnon sideband is $E_{2\sigma}$ ($\sim$25 310 cm^{-1}).[14] The zero-magnon line (M_σ) for the other magnon sideband $E_{1\sigma}$ ($\sim$25 302 cm^{-1}) is active only for $\mathbf{H} \parallel \mathbf{Z}$ and cannot be observed on this axial spectrum ($\mathbf{E} \perp \mathbf{Z}$, $\mathbf{H} \perp \mathbf{Z}$).[17]

MnF_2 has two sublattices, and it has two types of antiferromagnetic ordering distinguished by which sublattice is occupied by up spins and which by down. The crystal can be easily made to have a single antiferromagnetic phase by cooling it under a magnetic field that is slightly canted from the Z axis ($\sim 2^\circ$), having a small H_X but $H_Y = 0$.[6] The presence of the transverse magnetic field results in additional free energy $\mathcal{F}^{(HHHL)} \equiv \chi_{ijkl} H_i H_j H_k L_l$, where the nonlinear magnetic susceptibility tensor $\chi_{ZXXZ} = -\chi_{ZYYZ}$ is nonzero for the crystals belonging to the magnetic point group $4'/mmm'$. This free-energy term is odd with respect to the antiferromagnetic order parameter and to the external magnetic field. Therefore, one particular order can be chosen by the sign of the external magnetic field during the field-cooling process.

To observe the magnetic field dependence of the dichroism, a static magnetic field from -5 to $+5$ T was applied along the Z axis. The spatiotemporal symmetry of the crystal restricts the MLD to be odd with respect to $\mathbf{L}$, whereas the MCD should be even. Hence, we antisymmetrized the MLD data between two opposite antiferromagnetic orderings to extract pure MLD, and symmetrized the MCD data. In addition, their zero-field values were subtracted to remove residual signals from defects or a slight distortion of the crystal.[18] Figures 2(b) and 2(c) show the magnetic field dependence of the MLD and MCD after these procedures. Their slopes over the range of magnetic field values are also shown in Fig. 2(d).

There are several noticeable features in the experimental observations, as shown in Fig. 2(d). (i) A strong MLD appeared at the higher edge of the magnon sideband, but its MCD was almost negligible. (ii) The MLD spectra exhibited a step at the lower edge of the magnon sideband. (iii) A weaker feature was found in the MLD spectra, which looked like it was a derivative of the magnon sideband $E_{1\sigma}$. (iv) The magnetic dipole line (M_π) was split under a magnetic field, which caused both the MLD and MCD to have similar strengths.

III. ZEEMAN SHIFTS OF THE EXCITONS AND MAGNONS

In this section, we explain the experimentally obtained features of the magneto-optical phenomena of MnF_2 based on microscopic theories of optical absorption. First, we believe

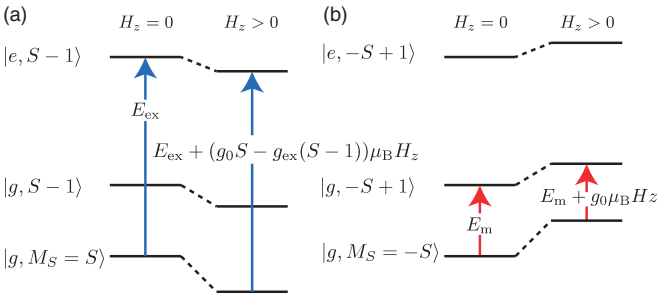

FIG. 3. (Color online) Zeeman shifts in the energies of (a) an exciton in sublattice A and (b) a magnon in sublattice B. g and e denote the orbital functions of the ground and the excited states, respectively.

that the change in absorption coefficients under a magnetic field at low temperature is mainly due to Zeeman shifts of the absorption lines.[19] For example, the MLD and MCD around the (M_π) line strongly indicate that their origin is the Zeeman split of an exciton, $2\gamma_{\rm ex} H_z \equiv 2[g_{\rm ex} S - g_0(S-1)]\mu_{\rm B} H_z$, and is proportional to the external magnetic field. g_0 and $g_{\rm ex}$ are g factors of the ground and excited states, respectively. $S = 5/2$ is the ion spin and $\mu_{\rm B}$ is the Bohr magneton. Because the ground state, ${}^6A_{1g}$ of Mn^{2+}, is an orbital singlet, its g factor can be considered as that of an electron spin, i.e., $g_0 = 2$.[20] The value of $g_{\rm ex}$ was determined to be 1.89 ± 0.01 on the basis of this splitting.

The effective Zeeman splitting of the exciton magnon pair creation is much smaller than that of an exciton line. This is because the exciton and the magnon are created in opposite sublattices so that total spin is conserved. For example, consider that sublattice A is occupied by up spins (M_S, z component of the ion spin, is S) and sublattice B by down spins ($M_S = -S$). When an exciton is created in sublattice A, the electronic state of an ion is excited from the ground state with $M_S = S$ to an excited state with $M_S = S - 1$. On the other hand, the creation of a magnon in sublattice B (down spin sites) increases the M_S of an ion from $-S$ to $-S+1$, while its orbital function remains unchanged from its ground state. Under an external magnetic field along the z axis, the energies of the exciton [$E^{\rm A}_{\rm ex}(H_z)$] and the magnon [$E^{\rm B}_{\rm m}(H_z)$] change depending on the g factors of the ground (g_0) and the excited ($g_{\rm ex}$) states:

$$E^{\rm A}_{\rm ex}(H_z) = E^{\rm A}_{\rm ex}(0) + [g_0 S - g_{\rm ex}(S-1)]\mu_{\rm B} H_z, \quad (1)$$

$$E^{\rm B}_{\rm m}(H_z) = E^{\rm B}_{\rm m}(0) + g_0 \mu_{\rm B} H_z, \quad (2)$$

The total energy of this pair-creation process thus changes by $\gamma_{\rm eff} H_z \equiv (g_0 - g_{\rm ex})(S-1)\mu_B H_z$, as depicted in Fig. 3.

In the following sections, we derive how these Zeeman splittings result in the observed magneto-optical properties of MnF_2 by considering the polarization selection rules of the corresponding transitions.

IV. POLARIZATION SELECTION RULES FOR MAGNON SIDEBANDS

In this section, we derive the polarization selection rules for the magnon-sideband absorption. In the literatures, there

are several ways to obtain the line shapes of the magnon sidebands,[17,21–23] but none considers the magnetic field induced dichroism; hence, we extend these theories to consider the dichroism. We start with the effective electric polarization operator **P** created by the exciton magnon pair:[15]

$$\mathbf{P} = \sum_{\substack{\langle i\in A,\, j\in B\rangle \\ l=0 \text{ to } 3}} [\boldsymbol{\pi}^{(i(l),j)}\alpha_i^\dagger S_j^+ + \boldsymbol{\pi}^{(j(l),i)}\alpha_j^\dagger S_i^-], \tag{3}$$

where $\alpha_i^\dagger$ is the creation operator of an exciton at a site i, and $S_j^\pm$ is the spin ladder operator on a site j. The sum is taken over neighboring pairs $\langle i \in A, j \in B\rangle$. The superscripts $i(l)$ and $j(l)$ indicate that the orbital of the electronic excitation behaves as B_{lg} of D_{2h} for $l = 1,2,3$, while it behaves as A_g with $l = 0$. We employ the (X,Y,Z) coordinate system (depicted in Fig. 1) for D_{2h}, whose character table is shown in Table I. Note that the exciton orbitals always have even parity, and these four representations are sufficient to consider all the possible orbitals.

A symmetry consideration simplifies the form of this operator.[21] The total spin is conserved in this pair creation, which enables us to use the spatial site symmetry D_{2h}, instead of the corresponding double group. For example, an exciton with the orbital representation of A_g (i.e., invariant under any symmetry operation of D_{2h}) contributes to P_X through the B_{3u} component of $\pi_X^{(i(0),j)}$. This is because P_X behaves as B_{3u} in D_{2h} and it is only the product of A_g and B_{3u} that contains B_{3u}, which can be easily verified from the character table. Similarly, the B_{2u} component of $\pi_X^{(i(1),j)}$ contributes to P_X because the B_{1g} (orbital of the exciton) $\times$ $B_{2u} = B_{3u}$. In this way, when $\boldsymbol{\pi}^{(i(l),j)}$ is decomposed into irreducible representations of D_{2h}, only limited components remain nonzero.

To construct the basis functions of these irreducible representations, we introduce the function $\sigma_k^{ij} \equiv \mathrm{sgn}\left[(\mathbf{r}_j)_k - (\mathbf{r}_i)_k\right]$, where the superscript j covers all eight neighbors surrounding an ion i. These eight neighbors are categorized as type I or II depending on whether the ions are equivalent under the operations of D_{2h}, as illustrated in Fig. 1. Note that $\pi_X^{(i(l),j)}$ is the function for the choice of neighboring pairs, $\langle i,j\rangle$, for a fixed l. When we use the (X,Y,Z) coordinate system, only type-I neighbors contribute to σ_Y^{ij}, whereas type-II neighbors appear in σ_X^{ij}. To clarify this situation, we write them as $\sigma^{ij}(\mathrm{I})_Y$ and $\sigma^{ij}(\mathrm{II})_X$, and they are basis function of B_{2u} and B_{3u}, respectively.

Consequently, the X and Y components of $\boldsymbol{\pi}^{(i(l),j)}$ are described as

$$\pi_X^{(i(l),j)} = \pi_X^{(1)}(\mathrm{I})\sigma^{ij}(\mathrm{I})_Y + \pi_X^{(0)}(\mathrm{II})\sigma^{ij}(\mathrm{II})_X, \tag{4}$$

$$\pi_Y^{(i(l),j)} = \pi_Y^{(0)}(\mathrm{I})\sigma^{ij}(\mathrm{I})_Y + \pi_Y^{(1)}(\mathrm{II})\sigma^{ij}(\mathrm{II})_X, \tag{5}$$

where $\pi_X^{(l)}(\mathrm{I\ or\ II})$ are the coefficients of the linear combinations. Note that the cross terms between the two sets of representations, (A_g, B_{1g}) and (B_{2g}, B_{3g}), vanish in the magnon-sideband absorption because excitons at different zone boundaries contribute to the magnon sidebands.[17] Hence, we first deal with A_g and B_{1g}, and leave the other set aside.

The two sublattices are transformed into each other by a π rotation around the x axis or y axis, and thus $\boldsymbol{\pi}^{(j(l),i)}$ can be obtained by these rotations. In addition, the crystal as a whole should be invariant under an antiunitary operation θC_{4z}. Other symmetry operations of the magnetic point group do not add further constraints. As a result, the effective polarization operator is given by

$$\begin{aligned} P_x &= \sum_{\langle i,j\rangle} \left(I\sigma_x^{ij} + J\sigma_y^{ij}\right)\alpha_i^\dagger S_j^+ + \left(-I\sigma_x^{ij} + J\sigma_y^{ij}\right)\alpha_j^\dagger S_i^-, \\ P_y &= \sum_{\langle i,j\rangle} \left(J^*\sigma_x^{ij} + I^*\sigma_y^{ij}\right)\alpha_i^\dagger S_j^+ + \left(J^*\sigma_x^{ij} - I^*\sigma_y^{ij}\right)\alpha_j^\dagger S_i^-, \end{aligned} \tag{6}$$

where $\sigma_x^{ij} \equiv \sigma^{ij}(\mathrm{I})_Y + \sigma^{ij}(\mathrm{II})_X$ and $\sigma_y^{ij} \equiv \sigma^{ij}(\mathrm{I})_Y - \sigma^{ij}(\mathrm{II})_X$. I and J are complex values defined by

$$\begin{bmatrix} I \\ I^* \\ J \\ J^* \end{bmatrix} = \frac{1}{2\sqrt{2}} \begin{bmatrix} \pi_Y^{(0)}(\mathrm{I}) + \pi_X^{(0)}(\mathrm{II}) + \pi_X^{(1)}(\mathrm{I}) + \pi_Y^{(1)}(\mathrm{II}) \\ \pi_Y^{(0)}(\mathrm{I}) + \pi_X^{(0)}(\mathrm{II}) - \pi_X^{(1)}(\mathrm{I}) - \pi_Y^{(1)}(\mathrm{II}) \\ \pi_Y^{(0)}(\mathrm{I}) - \pi_X^{(0)}(\mathrm{II}) + \pi_X^{(1)}(\mathrm{I}) - \pi_Y^{(1)}(\mathrm{II}) \\ \pi_Y^{(0)}(\mathrm{I}) - \pi_X^{(0)}(\mathrm{II}) - \pi_X^{(1)}(\mathrm{I}) + \pi_Y^{(1)}(\mathrm{II}) \end{bmatrix}. \tag{7}$$

TABLE I. Character table for D_{2h}. E is the identity, C_{2i} is the rotation by π around i axis, and I is the inversion. The rows σ_h, σ_{vY}, and σ_{vX} represent mirror operations with respect to XY, ZX, and YZ planes, respectively. The corresponding basis functions are also described in terms of linear, rotational, and quadratic functions of the coordinates. Electric and magnetic fields behave as linear and rotational functions, respectively.

	A_g	B_{1g}	B_{2g}	B_{3g}	A_u	B_{1u}	B_{2u}	B_{3u}
E	1	1	1	1	1	1	1	1
C_{2Z}	1	1	−1	−1	1	1	−1	−1
C_{2Y}	1	−1	1	−1	1	−1	1	−1
C_{2X}	1	−1	−1	1	1	−1	−1	1
I	1	1	1	1	−1	−1	−1	−1
σ_h	1	1	−1	−1	−1	−1	1	1
σ_{vY}	1	−1	1	−1	−1	1	−1	1
σ_{vX}	1	−1	−1	1	−1	1	1	−1
Linear (**E**)						Z	Y	X
Rotation (**H**)		R_Z	R_Y	R_X				
Quadratic	X^2, Y^2, Z^2	XY	ZX	YZ				

The absorption coefficient matrix K in the xy plane is obtained by Eq. (6) through a standard method using Fermi's "golden rule":[17]

$$K(\omega) = \begin{bmatrix} |I|^2+|J|^2 & 2I^*J^* \\ 2IJ & |I|^2+|J|^2 \end{bmatrix} L_1(\omega - \gamma_{\rm eff}H_z) + \begin{bmatrix} |I|^2+|J|^2 & -2I^*J^* \\ -2IJ & |I|^2+|J|^2 \end{bmatrix} L_1(\omega + \gamma_{\rm eff}H_z), \quad (8)$$

where L_1 is the line-shape function of the magnon sidebands given on the basis of the dispersions of the excitons and magnons. Note that the crystal coordinate system, (x,y,z), is employed here. The two terms are magnon sidebands corresponding to $\alpha_i^\dagger S_j^+$ and $\alpha_j^\dagger S_i^-$, respectively.

When $H_z = 0$, the two sidebands in Eq. (8) are degenerate; the crystal is uniaxial. This is consistent with previous studies. However, an external magnetic field lifts this degeneracy through the Zeeman shifts $\pm\gamma_{\rm eff}H_z$. This results in the off-diagonal terms of the absorption coefficient matrix, i.e., the dichroism. Namely, the real and imaginary parts of IJ cause the MLD and MCD, respectively.

When the exciton orbital behaves as pure A_g, I and J are real values because $I = I^*$ and $J = J^*$ according to Eq. (7). Similarly, if it is pure B_{1g}, I and J are purely imaginary. In both cases, IJ is a real value, and only the MLD is allowed.

To make the MCD of the magnon sideband allowed, the exciton should have both A_g and B_{1g} characters. This is achieved through the mixing of A_g and B_{1g} excitons by spin-orbit coupling. In the case of the C line, the corresponding excited state is $({}^4A_{1g},{}^4E_{1g})$, and the orbital of the exciton contains A_g and has no B_{1g} component. Only when two excited states with these characters are energetically close, specifically when their energy difference is smaller than the energies of the spin-orbit interactions, do they mix with a considerable amplitude. Thus, only the MLD is allowed and the MCD is prohibited for the magnon sidebands of the C line.

A similar reasoning is available for B_{2g} and B_{3g} excitons: only when the exciton has both B_{2g} and B_{3g} characters is the MCD allowed. An example of such a transition having both B_{2g} and B_{3g} is the A line $({}^6A_{1g} \rightarrow {}^4T_{1g})$ of MnF_2. Thus, it has been reported that the MCD can stem from the magnon sidebands of this transition (the A line).[6] On the other hand, $({}^4A_{1g},{}^4E_{1g})$ contains only B_{3g} but not B_{2g}, and the MCD should be absent. In this way, whether the magnon sidebands of an exciton can exhibit MCD can be easily determined by which representations in D_{2h} are involved in the multiplet of O_h, as summarized in Table II.

TABLE II. Correlations between the representations of D_{2h} and O_h site symmetries, and the resulting selection rules for MLD and MCD. Note that the coordinates depicted in Fig. 1 are used.

O_h	A_g or B_{1g}	B_{2g} or B_{3g}
A_{1g}	A_g (MLD)	
A_{2g}		B_{3g} (MLD)
E_g	A_g (MLD)	B_{3g} (MLD)
T_{1g}	B_{1g} (MLD)	$B_{2g}+B_{3g}$ (MLD + MCD)
T_{2g}	A_g+B_{1g} (MLD + MCD)	B_{2g} (MLD)

V. POLARIZATION SELECTION RULES FOR MAGNETIC DIPOLE TRANSITIONS

Unlike the case of the magnon sidebands, both the MLD and MCD are always allowed by symmetry for the magnetic dipole transition M_π. This is because the single ionic excitations from the high-spin d^5 configuration require a change in spin by ±1, hence the magnetic dipole transition inherently requires spin-orbit coupling to make it spin allowed.[13] Therefore, the orbital and the spin of an exciton cannot be treated separately. The site symmetries should be taken as the double group of C_{2h}, and the selection rules are given according to this group.[17,24] For example, single ionic excitations with orbital functions of A_g or B_{1g} can be excited by the magnetic-field component of light in the x-y plane. This is because these excitons belong to ${\Gamma_2}^+$ of C_{2h},[17] and both H_x and H_y belong to the same representation. The magnetic dipole operators μ_x and μ_y should be invariant under the allowed space-time symmetry operations of MnF_2. As a result, they are described by the creation operators $\alpha_i^\dagger$ and $\alpha_j^\dagger$ (i and j represent sites in sublattices A and B, respectively) of the single ionic excitations:

$$\mu_x = \sum_{i\in A} C\alpha_i^\dagger + \sum_{j\in B} -C^*\alpha_j^\dagger, \quad (9)$$

$$\mu_y = \sum_{i\in A} C^*\alpha_i^\dagger + \sum_{j\in B} C\alpha_j^\dagger. \quad (10)$$

The corresponding absorption coefficient matrix is

$$K_{{\rm ex}\perp}(\omega) \propto \begin{bmatrix} |C|^2 & C^{2*} \\ C^2 & |C|^2 \end{bmatrix} \delta(\hbar\omega - E_{\rm ex} + \gamma_{\rm ex}H_z) + \begin{bmatrix} |C|^2 & -C^{2*} \\ -C^2 & |C|^2 \end{bmatrix} \delta(\hbar\omega - E_{\rm ex} - \gamma_{\rm ex}H_z). \quad (11)$$

Without an external magnetic field, these two absorption lines are degenerate, and the off-diagonal terms cancel each other, which results in isotropic in-plane absorption. The real part of C^2 changes the symmetric component of the absorption coefficient tensor. Thus, MLD occurs. On the other hand, its imaginary part modifies the antisymmetric components of the absorption coefficient tensor, resulting in MCD. Because C is a general complex value, both MLD and MCD are allowed.

VI. COMPARISON OF THEORY WITH EXPERIMENT

Finally, we calculate the MLD and MCD spectra of the C line on the basis of the above selection rules. Figures 2(f) and 2(g) show the calculated spectra of the MLD and MCD as functions of the external magnetic field, and Fig. 2(h) plots their slopes over the field.

As previously discussed, the polarization eigenstates of the light fields for the magnon-sideband absorption are two cross-linear polarizations. We employed the absorption line shapes calculated by Meltzer *et al.*,[14] as reproduced in Fig. 2(e). These resonances are degenerate without an external magnetic field. Under a magnetic field H_z along the z axis, their energies split by $2\gamma_{\rm eff}H_z \equiv (g_0 - g_{\rm ex})(S-1)\mu_B H_z$. This determines the spectral shape of the MLD corresponding to the magnon sidebands.

For the C line, there is one magnon sideband (E_π) for the M_π exciton and two sidebands ($E_{1\sigma a}$ and $E_{1\sigma b}$) for the M_σ.

The g factors of the ground and excited states determine the size of splitting. The ground state is an orbital singlet, and thus one can assume $g_0 = 2$ as its g factor. The excited state for the M_π exciton has $g_{\rm ex} = 1.89$, as experimentally determined from the splitting of the magnetic dipole line in this study. For the M_σ exciton, we employed the value of $g_{\rm ex} = 1.96$ that was determined by Meltzer *et al.*[13] For the magnetic dipole transition to directly create excitons, one cannot determine the strength of the MLD or the MCD. We assumed that they have the same amplitude, which agrees well with the experiment.

The calculated spectra show excellent agreement with the experiments: all the four important features in Fig. 2(d) are reproduced by the calculation. Both (i) the strong peak in the MLD at the higher energy shoulder and (ii) the step in the MLD at the lower-energy shoulder were explained on the basis of the Zeeman split of the magnon sideband, reflecting the asymmetric line-shape function of the magnon sideband. (iii) The Zeeman split of $E_{1\sigma a}$ and $E_{2\sigma b}$ well explains the line shape of the MLD observed around 25 300 $\rm cm^{-1}$. (iv) Both the MCD and MLD originate from the magnetic dipole transition M_π. The clear agreement between the experiments and calculations strongly supports the selection rules for dichroism under an external magnetic field.

Note that a very weak MCD at the $E_{2\sigma}^{\rm high}$ edge of the magnon sideband was observed during the experiments, which seemingly contradicts the above theory. This can be explained as a slight mixing between the different multiplet states of O_h by the spin-orbit interaction, which is neglected in the discussion above. In the case of the C line, we assumed that the ground state is purely ${}^6A_{1g}$ and the excited state is ${}^4A_{1g}$ and ${}^4E_{1g}$. This assumption led to the conclusion that the orbital of an exciton cannot be a mixture of A_g and B_{1g} of the D_{2h} representations, and only MLD is allowed. However, the spin-orbit interaction mixes different multiplets of O_h: for example, the ground state contains the ${}^4T_{1g}$ character in addition to the ${}^6A_{1g}$. Therefore, the orbital function of an exciton contains a T_{1g} part in terms of O_h because $T_{1g} \times A_{1g} = T_{1g}$. Hence, this orbital function contains both A_g and B_{1g} of D_{2h}, which allows MCD of this resonance. Yet, such intermultiplet mixing should be much smaller than intramultiplet mixing because multiplets of O_h are well separated in energy ($>$1000 $\rm cm^{-1}$), which explains why the MCD of the C-line magnon sideband almost vanishes.

VII. SUMMARY

In summary, we revealed the microscopic nature of the magneto-optical phenomena of the C line of MnF_2 through systematic experiments and group-theoretical analysis. In this material, the creation of a pair of a magnon and an exciton, i.e., magnon-sideband absorption, provides the strongest oscillator strength among a number of absorption mechanisms. An external magnetic field lifts the degeneracy between the two otherwise degenerate magnon sidebands. We theoretically demonstrated that the polarization eigenstates of light that are absorbed by these sidebands are two cross-linear polarizations, not circular polarizations. This explains why this sideband shows dichroism for two cross-linear polarizations under an external field, i.e., MLD, whereas the normal MCD vanishes.

When magneto-optical phenomena are considered, it is widely accepted that they involve atomic transitions in a free space. In this case, angular momentum is a better quantum number to use in order to label the atomic states. Hence, selection rules based on circular polarizations are useful based on the change in angular momentum of atomic states as a result of light absorption. In particular, an external magnetic field lifts the degeneracy between different angular momentum states, which results in MCD.[19] Even in the case of magnetically ordered crystals, which is specifically important for a number of applications, the role of crystalline symmetry is usually taken as an additional perturbation to this considerations of atomic transitions.

However, in this study, we highlight that solids may require a more careful treatment of their crystalline symmetry by showing an example where such a perturbative extension is invalid. Namely, the magnon sideband of the C line of MnF_2 did not show the MCD, while the MLD was observed, which strongly differs from the magneto-optical property of a single Mn^{2+} ion in free space. This is because two different ions contribute to the magnon sideband absorption, and crystalline symmetry plays a key role in such nonlocal phenomena. We believe that proactive usage of such crystalline symmetry provides a new direction for utilizing light as a tool to probe and control magnetism. In particular, the MLD discussed in this study has a highly unique potential for handling the magnetic properties of solids, for example, controlling the antiferromagnetic order parameter by light.

ACKNOWLEDGMENTS

The authors acknowledge N. Nagasawa and Tokuyama Co. for providing the MnF_2 crystal, Y. Svirko for his careful reading of the manuscript, and appreciate Y. Tanabe and H. Tamaru for their helpful discussions. This work was supported partly by a Grant-in-Aid for Scientific Research (KAKENHI) on Innovative Areas "Optical Science of Dynamically Correlated Electrons (DYCE, Grant No. 2003)" (20104002) of Ministry of Education, Culture, Sports, Science, and Technology of Japan (MEXT), and JSPS through its FIRST Program. T.H. acknowledges support by Grant-in-Aid for JSPS Fellows.

[1] A. Kirilyuk, A. V. Kimel, and T. Rasing, Rev. Mod. Phys. **82**, 2731 (2010).
[2] P. S. Pershan, J. Appl. Phys. **38**, 1482 (1967).
[3] L. Landau and E. Lifshitz, *Electrodynamics of Continuous Media* (Butterworth-Heinemann, Oxford, 1984).
[4] A. P. Cracknell, Rep. Prog. Phys. **32**, 633 (1969).
[5] V. V. Eremenko, N. F. Kharchenko, Y. G. Litvinenko, and V. M. Naumenko, *Magneto-optics and Spectroscopy of Antiferromagnets* (Springer-Verlag, New York, 1992).
[6] N. F. Kharchenko, O. V. Miloslavskaya, and A. A. Milner, Low Temp. Phys. **31**, 825 (2005).
[7] J. W. Stout and S. A. Reed, J. Am. Chem. Soc. **76**, 5279 (1954).

[8]F. M. Johnson and A. H. Nethercot, Phys. Rev. **114**, 705 (1959).
[9]F. L. Scarpace, M. Y. Chen, and W. M. Yen, J. Appl. Phys. **42**, 1655 (1971).
[10]R. W. Schwartz, J. A. Spencer, W. C. Yeakel, P. N. Schatz, and W. G. Maisch, J. Chem. Phys. **60**, 2598 (1974).
[11]J. W. Stout, J. Chem. Phys. **31**, 709 (1959).
[12]J. W. W. Parkinson and F. E. Williams, J. Chem. Phys. **18**, 534 (1950).
[13]R. S. Meltzer and J. L. L. Lohr, J. Chem. Phys. **49**, 541 (1968).
[14]R. S. Meltzer, M. Lowe, and D. S. McClure, Phys. Rev. **180**, 561 (1969).
[15]Y. Tanabe, T. Moriya, and S. Sugano, Phys. Rev. Lett. **15**, 1023 (1965).
[16]R. L. Greene, D. D. Sell, W. M. Yen, A. L. Schawlow, and R. M. White, Phys. Rev. Lett. **15**, 656 (1965).
[17]R. Loudon, Adv. Phys. **17**, 243 (1968).
[18]Y. H. Wong, F. L. Scarpace, C. D. Pfeifer, and W. M. Yen, Phys. Rev. B **9**, 3086 (1974).
[19]P. N. Schatz and A. J. McCaffery, Q. Rev. Chem. Soc. **23**, 552 (1969).
[20]P. G. Russell, D. S. McClure, and J. W. Stout, Phys. Rev. Lett. **16**, 176 (1966).
[21]Y. Tanabe and K.-I. Gondaira, J. Phys. Soc. Jpn. **22**, 573 (1967).
[22]Y. Tanabe and K. Aoyagi, in *Excitons*, edited by E. I. Rashba and M. D. Sturge (North-Holland, New York, 1982), pp. 603–663.
[23]D. D. Sell, R. L. Greene, and R. M. White, Phys. Rev. **158**, 489 (1967).
[24]J. O. Dimmock and R. G. Wheeler, Phys. Rev. **127**, 391 (1962).